

## Influence of shape on electron transport in ballistic quantum dots

M. J. Berry, J. A. Katine, and R. M. Westervelt

*Division of Applied Sciences and Department of Physics, Harvard University, Cambridge, Massachusetts 02138*

A. C. Gossard

*Materials Department, University of California, Santa Barbara, California 93110*

(Received 29 August 1994)

We have investigated the low-temperature ( $T=0.43\text{--}4.25$  K) magnetotransport of quantum dots fabricated in the shape of an open circle and a circle having a central bar. The characteristic magnetic fields for both coherent backscattering and conductance fluctuations are strongly shape dependent: both are larger by a factor  $\approx 3$  in the device with the central bar. Comparison of large and small devices of nominally identical shape shows that characteristic trajectory areas are proportional to the device area.

Mesoscopic transport in diffusively scattering metals and metallic semiconductors has been carefully studied:<sup>1</sup> interference of forward-scattered electron waves traveling by different paths causes time-independent conductance fluctuations; interference of time-reversed pairs of backscattered electron waves leads to weak localization. Analogs of both phenomena have recently been observed in ballistic microstructures for which the mean free path greatly exceeds the size of the device. At low temperatures, the magnetoconductance of circular and stadium-shaped quantum dots with quantum point contacts show conductance fluctuations due to the interference of electron waves traveling between the contacts by different paths,<sup>2</sup> and a coherent backscattering peak at zero magnetic field due to the interference of time-reversed pairs of backscattered trajectories.<sup>2-6</sup>

Quantum interference phenomena in ballistic microstructures are of great interest because they are produced by scattering from the walls of the structure rather than by randomly located impurities and are thus inherently shape dependent, and because they make contact with the fundamental theory of statistical mechanics and quantum chaos in billiards.<sup>7</sup> A circular billiard differs from a stadium in that an ideal circle

has integrable trajectories that conserve angular momentum, while an ideal stadium produces chaos. The differences observed between circles and stadia in measurements of conductance fluctuations and coherent backscattering are, however, not large and require quantitative analysis to discern.<sup>2-5</sup> The lack of obvious differences between data from circles and stadia may in part be due to the redirection of electron trajectories by the small-angle scattering and boundary roughness present to some degree in all samples.<sup>8</sup>

In this paper we present magnetoresistance data on quantum dots fabricated in the shapes of an open circle and a circle with a barrier between the point contacts, which show large, unambiguous shape- and size-dependent changes in both the conductance fluctuation spectra and the coherent backscattering peak. Figures 1(a) and 1(b) show electron micrographs of quantum dots with quantum point contacts fabricated in two shapes: shape A, an open circle and shape B, a circle with a central barrier; the bright area is a patterned Au gate used to define the dot in a two-dimensional electron gas located underneath the gate in a GaAs/Al<sub>x</sub>Ga<sub>1-x</sub>As heterostructure. Conductance fluctuations originate from interference of forward-scattered electron waves as indicated for

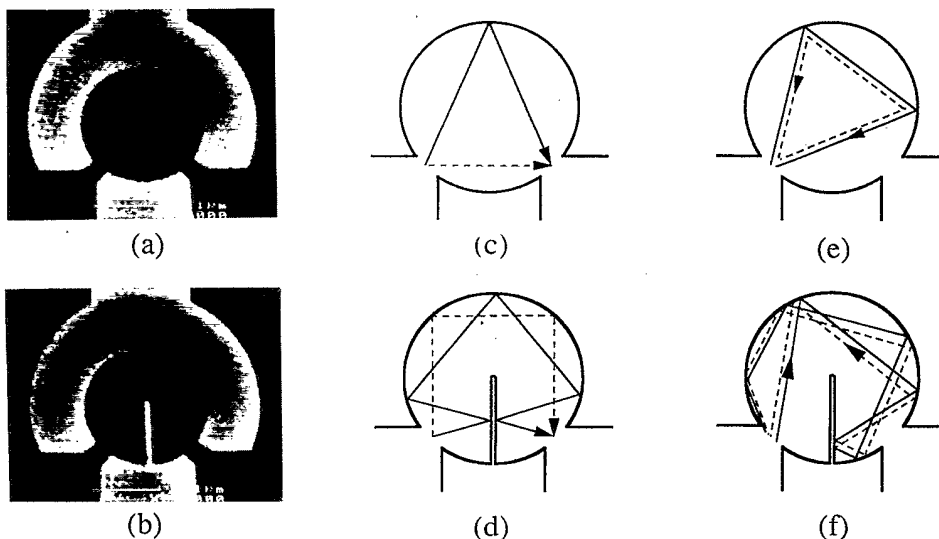


FIG. 1. Scanning electron microscopy micrographs of (a) large-shape A and (b) large-shape B; length bar is  $1\ \mu\text{m}$ . In shape A, forward-scattered (c) and backscattered (e) trajectories circulate in a single direction; in shape B [(d) and (f)], they reverse direction with each rebound off the central bar, partially canceling the accumulated area. Trajectories circulating clockwise (counterclockwise) are shown in solid (dashed) lines.

the open circle in Fig. 1(c), while coherent backscattering originates from the interference of pairs of time-reversed paths as shown in Fig. 1(e). For the same device, the enclosed area for coherent backscattering is larger than that for conductance fluctuations by roughly a factor of 2. Characteristic areas can be measured experimentally via the magnetic field necessary to insert a fraction of a flux quantum,  $\Phi_0/2\pi = \hbar/e$ , and thereby change the interference. For open circular dots, electrons circulate in the same direction, and the enclosed areas can be quite large.

As illustrated in Figs. 1(d) and 1(f), the barrier in shape *B* reflects electron trajectories and greatly reduces the enclosed area of both forward-scattered trajectories linking the two contacts, as well as the enclosed area of time-reversed pairs of backscattered trajectories. Thus we expect the characteristic areas associated with conductance fluctuations and coherent backscattering in shape *B* to be smaller than for the open circle, and the corresponding characteristic magnetic-field scales to be larger. This difference should be robust to small amounts of disorder: although small-angle scattering and boundary roughness destroy the perfect symmetry of the open circle, they are unlikely to completely reverse the direction of circulation.

Quantum-dot devices were fabricated using electron-beam lithography and Cr/Au metallization to define gate structures on the surface of GaAs/Al<sub>x</sub>Ga<sub>1-x</sub>As heterostructures containing a two-dimensional electron gas with density  $n = 4.4 \times 10^{11} \text{ cm}^{-2}$  and mobility  $\mu = 350\,000 \text{ cm}^2/\text{V sec}$ , located  $420 \text{ \AA}$  below the surface. Two pairs of devices were made with nominally identical shapes; one large pair (pictured in Fig. 1) with electron-gas area  $\approx 1.6 \mu\text{m}^2$  obtained by subtracting the depletion width from the lithographic size, and one small pair (not shown) with electron gas area  $\approx 0.43 \mu\text{m}^2$ . The width of the bar in the devices with barriers is less than  $50 \text{ nm}$ . All four devices are much smaller than the measured mean free path  $3.8 \mu\text{m}$ , so electron trajectories inside the dots approximate straight lines, and we say that transport is ballistic. In our devices, the measured small-angle scattering time  $\tau_s \approx 0.5 \text{ psec}$ .<sup>9</sup> At  $0.43 \text{ K}$ , the measured phase coherence length was  $19 \mu\text{m}$  for ballistic motion.<sup>10</sup> The samples were cooled in a <sup>3</sup>He cryostat to temperatures between  $0.43$  and  $4.25 \text{ K}$ , inside a superconducting solenoid. The magnetic field was oriented perpendicular to the plane of the electron gas, and the precision of the field sweeps was  $\pm 0.01 \text{ mT}$ . Magnetoresistance measurements were made using ac lock-in techniques at  $11 \text{ Hz}$ .

Figure 2 shows four magnetoresistance plots taken at  $T = 0.43 \text{ K}$  that illustrate the striking difference between shapes *A* and *B*. Data for the large devices are shown as the upper (*B*) and lower (*A*) traces in Fig. 2(a), data for the smaller versions of the devices are shown in Fig. 2(b). All four magnetoresistance traces have the same qualitative features: a resistance peak centered at zero magnetic field due to coherent backscattering,<sup>2-6</sup> superimposed on conductance fluctuations due to interference of forward-scattered paths.<sup>2</sup> The magnetic-field scales for shapes *A* and *B*, however, are quite different. As predicted by theory, the width of the zero-field peak and the characteristic field for conductance fluctuations are both much larger for the circles with a barrier than the open circles. Comparing large and small devices of

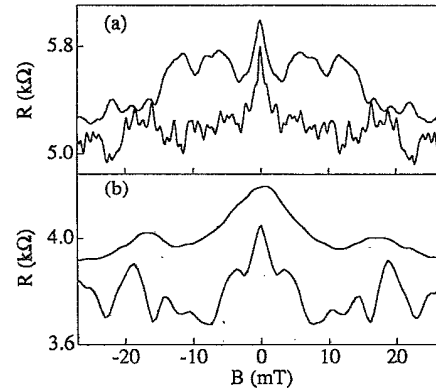


FIG. 2. Representative raw magnetoresistance data taken at  $T = 0.43 \text{ K}$  with (a) both large devices biased at  $-0.7 \text{ V}$  and (b) both small devices biased at  $V = -0.5 \text{ V}$ . Shape-*A* data (lower traces) offset for clarity from shape *B* (upper). Note more rapid oscillations and narrower zero-field peak in large vs small and in *A* vs *B*.

the same shape, we find that the magnetic-field scales are inversely proportional to the area of the electron gas, also in agreement with theory.

Figures 3(a)–3(d) show the resistance change  $\Delta R/R$  due to coherent backscattering (solid lines), averaged over five gate voltages, for all four devices at  $T = 0.43 \text{ K}$ . The zero-field resistance peaks are fit by the Lorentzian line shape predicted by chaotic scattering theory (dashed lines). The coherent backscattering peak is robust: we observed the resistance peak at all bias voltages and temperatures in all devices on five separate thermal cycles. For a given sweep, conductance fluctuations distort the zero-field peak shape. In order to average away the effect of the conductance fluctuations, data were taken at five gate voltages in the conducting regime ( $G_{\text{dot}} > e^2/h$ ) for all four devices at  $0.1000\text{-V}$  intervals. Chaotic scattering theory predicts that the conductance minima near zero field is a Lorentzian.<sup>11</sup>

$$G(B) = G(0) - \Delta G_0 / [1 + (B/B_c)^2], \quad (1)$$

where  $B_c$  is the half width at half maximum. As shown in Fig. 3, a Lorentzian fits our data well at  $T = 0.43 \text{ K}$ . The

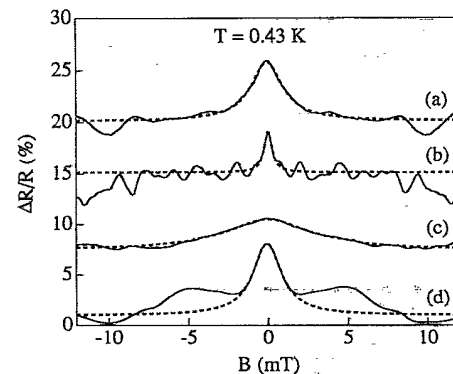


FIG. 3. Fractional change in magnetoresistance of (a) large-*B*-, (b) large-*A*-, (c) small-*B*-, and (d) small-*A*-shaped devices averaged over five gate voltages. Data (solid) are offset for clarity and fit to Lorentzian line shape (dashed).

TABLE I. Characteristic magnetic fields and corresponding enclosed trajectory areas for all devices at  $T=0.43$  K; values from chaotic theory fits of coherent-backscattering peak widths ( $B_c$ ) and power spectra of conductance fluctuations ( $B_\alpha$ ). Averaged over all four devices,  $A_c \cong 2.4 \pm 0.8 A_\alpha$ .

Size, shape	$B_c$ (mT)	$B_\alpha$ (mT)
	$A_c$ ( $\mu\text{m}^2$ )	$A_\alpha$ ( $\mu\text{m}^2$ )
Large, B	$1.2 \pm 0.2$	$2.2 \pm 0.4$
	$0.55 \pm 0.09$	$0.30 \pm 0.06$
Large, A	$0.30 \pm 0.06$	$0.80 \pm 0.12$
	$2.2 \pm 0.4$	$0.82 \pm 0.12$
Small, B	$3.4 \pm 0.7$	$7.8 \pm 1.2$
	$0.19 \pm 0.04$	$0.084 \pm 0.013$
Small, A	$1.1 \pm 0.2$	$2.6 \pm 0.4$
	$0.6 \pm 0.1$	$0.25 \pm 0.04$

predicted line shapes for devices A and B at zero temperature are more sharply peaked<sup>11,12</sup> due to the presence of large-area trajectories. Both small-angle scattering and the loss of phase coherence due to inelastic scattering at finite temperatures eliminate long trajectories that sharpen the peak shape in an integrable structure. Recently Chang *et al.*<sup>6</sup> found a Lorentzian line shape for the zero-field peak in an array of open circles at higher temperatures, and a more sharply peaked line shape for  $T < 0.4$  K.

Table I lists the half-width  $B_c$  of the coherent backscattering peak for all four devices, measured via the Lorentzian fits shown in Fig. 3, along with the corresponding trajectory areas  $A_c = \Phi_0/2\pi B_c$ . The error in  $B_c$  ( $\sim 20\%$ ) is dominated by uncertainty in the base line, whose value was a free parameter in the fit. Comparing the characteristic areas of shapes A and B, we find that the area  $A_c$  of the open circle is larger for both the large and small devices by factors 3.9 and 3.1, respectively. Comparing the characteristic areas  $A_c$  of large and small devices of the same shape, we find that the ratio for the large  $A_c$  to small is 3.6 to 1 for shape A and 2.9 to 1 for shape B, in good agreement with the  $\cong 3.7$  to 1 ratios for the electron-gas area in both shapes.

The characteristic area  $A_\alpha$  enclosed by pairs of forward-scattered paths leading to conductance fluctuations can be measured via power spectra of the resistance vs magnetic-field data. For chaotic systems, semiclassical analysis<sup>13</sup> predicts that the power spectrum  $S(f)$  of conductance fluctuations vs magnetic frequency  $f$  (cycles/T) is

$$S(f) = S_0(1 + 2\pi B_\alpha f) \exp(-2\pi B_\alpha f), \quad (2)$$

where  $B_\alpha$  is the magnetic-field change necessary to increase the flux through the characteristic area  $A_\alpha = \Phi_0/2\pi B_\alpha$  by  $\Phi_0/2\pi$ . For the open circle, no analytic form for the power spectrum corresponding to Eq. (2) exists; numerical results<sup>8,11</sup> give spectra with more power at higher magnetic frequencies, which resemble power laws. For consistency with our coherent-backscattering analysis, we use Eq. (2) to fit data for all four devices, despite the fact that we expect deviations from this form.

Figure 4 shows measured average power spectra of the conductance fluctuations vs magnetic frequency  $f$  in the

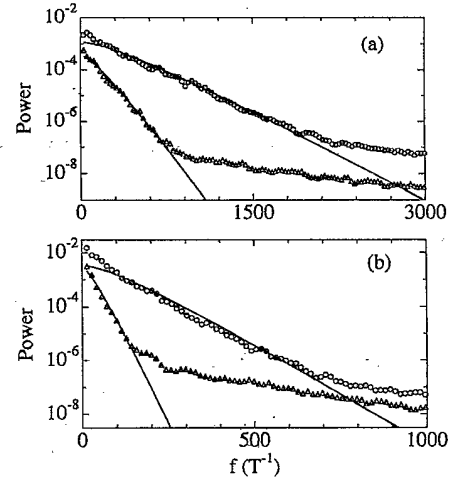


FIG. 4. Power spectra of conductance fluctuations for (a) large and (b) small devices vs magnetic frequency, averaged over five gate voltages. Data for shape A (circles) and shape B (triangles) are offset for clarity. Curve fits to Eq. (2) (solid) agree with data over four orders of magnitude in power. Note discrepancy between fit and data for both open circles at low  $f$ . The tail at high  $f$  is a noise effect.

large [Fig. 4(a)] and small [Fig. 4(b)] shape-A (circles) and shape-B (triangles) devices; the power spectra for shape-B devices have been offset downward by a decade for clarity. The solid lines in Fig. 4 are fits to theory [Eq. (2)]. These power spectra were obtained from low-field ( $|B| < 0.3$  and  $|B| < 0.5$  T for the small and large devices, respectively) magnetoconductance data to minimize the effects of trajectory curvature. A fourth-order polynomial was subtracted from each magnetic-field sweep to remove background magnetoconductance associated with the point contacts. As for the coherent-backscattering analysis above, power spectra were averaged over five gate voltages. At each gate voltage, 31 half-overlapping power-spectra segments were logarithmically averaged to suppress sharp structure at low frequencies associated with periodic orbits.

As shown in Fig. 4, chaotic theory provides a good fit to the conductance-fluctuation power spectra for the circles with barriers, suggesting that orbits within the actual devices are chaotic.<sup>14</sup> The fit for data from the open circular devices is less good: the power spectra for both circular devices are concave up, in agreement with numerical simulations<sup>8</sup> for open circular devices, whereas the power spectra predicted by chaotic theory are concave down. Nonetheless, the fit provides a good operational definition of a characteristic area  $A_\alpha$ , which quantifies the large differences in power spectra between the two device shapes in Figs. 4(a) and 4(b).

Table I summarizes the fitted characteristic fields  $B_\alpha$  and characteristic areas  $A_\alpha$  for the data of Fig. 4; the estimated error ( $\sim 15\%$ ) is largely due to uncertainty in the high-magnetic-frequency cutoff chosen for the fits. Comparing conductance fluctuations in our devices we find ratios of characteristic area  $A_\alpha$  for shapes A to B of 2.8:1 and 2.9:1 for large and small devices, respectively, and large-to-small  $A_\alpha$  ratios of 3.4:1 and 3.3:1 for shapes A and B, respectively. These ratios agree well with those obtained from our

coherent-backscattering analysis, suggesting that the electron trajectories contributing to both phenomena are similar. An important difference is that the characteristic area for coherent backscattering is expected to be approximately twice that for conductance fluctuations, because a *pair* of closed time-reversed paths are required for coherent backscattering. Averaging over all four devices, we find  $A_c \cong 2.4 \pm 0.8 A_\alpha$ , in good agreement with theory.

The authors thank Scott Yang, John Baskey, Doug Mar, and Mark Eriksson for help in conducting this experiment, and Harold Baranger, Charlie Marcus, and Douglas Stone for useful discussions. Two of us (M.J.B. and J.A.K.) acknowledge support from the Office of Naval Research. This work was supported at Harvard by ONR Grant No. N00014-89-J-1592 and NSF Grant No. DMR-91-19386, and at UCSB by Grant No. AFOSR-91-0214.

<sup>1</sup>Mesoscopic Phenomena in Solids, edited by B. L. Altshuler, P. A. Lee, and R. A. Webb (North-Holland, New York, 1991).

<sup>2</sup>C. M. Marcus, A. J. Rimberg, R. M. Westervelt, P. F. Hopkins, and A. C. Gossard, Phys. Rev. Lett. **69**, 506 (1992).

<sup>3</sup>M. J. Berry, J. H. Baskey, R. M. Westervelt, and A. C. Gossard, Phys. Rev. B **50**, 8857 (1994).

<sup>4</sup>M. J. Berry *et al.*, Surf. Sci. **305**, 495 (1994).

<sup>5</sup>M. W. Keller *et al.*, Surf. Sci. **305**, 501 (1994).

<sup>6</sup>A. M. Chang, H. U. Baranger, L. N. Pfeiffer, and K. W. West, Phys. Rev. Lett. **73**, 2111 (1994).

<sup>7</sup>M. C. Gutzwiller, *Chaos in Classical and Quantum Mechanics* (Springer, New York, 1990).

<sup>8</sup>W. A. Lin, J. B. Delos, and R. V. Jensen, Chaos **3**, 655 (1993).

<sup>9</sup>Shubnikov-de Haas oscillations measured at 430 mK were used to determine  $\tau$ , [J. P. Harring *et al.*, Phys. Rev. B **32**, 8442

(1985); F. Fang *et al.*, Surf. Sci. **196**, 310 (1988)].

<sup>10</sup>J. A. Katine, M. J. Berry, R. M. Westervelt, and A. C. Gossard, Superlatt. Microstruct. (to be published).

<sup>11</sup>H. U. Baranger, R. A. Jalabert, and A. D. Stone, in *Transport Phenomena in Mesoscopic Systems*, edited by H. Fukuyama and T. Ando (Springer, New York, 1992).

<sup>12</sup>H. U. Baranger, R. A. Jalabert, and A. D. Stone, Phys. Rev. Lett. **70**, 3876 (1993).

<sup>13</sup>R. A. Jalabert, H. U. Baranger, and A. D. Stone, Phys. Rev. Lett. **65**, 2442 (1990).

<sup>14</sup>Trajectories inside an ideal-shaped *B* device are integrable since they differ from those in an open circle by only a mirror reflection for each collision with the bar. Realistic devices with rounding of the bar and disorder are expected to possess chaotic orbits.